Journal of Scientific Research & Reports
12(6): 1-19, 2016; Article no.JSRR.26722
ISSN: 2320-0227

SCIENCEDOMAIN *international*
www.sciencedomain.org

Pollutants Spread in a Bifurcating River: The River Nun, Bayelsa, Nigeria

W. I. A. Okuyade[1*] and T. M. Abbey[2]

[1]Department of Mathematics and Statistics, University of Port Harcourt, Port Harcourt, Nigeria.
[2]Applied Mathematics and Theoretical Physics Group, Department of Physics, University of Port Harcourt, Port Harcourt, Nigeria.

Authors' contributions

This work was carried out in collaboration between both authors. Both authors read and approved the final manuscript.

Article Information

DOI: 10.9734/JSRR/2016/26722
Editor(s):
(1) Grigorios L. Kyriakopoulos, School of Electrical and Computer Engineering, National Technical University of Athens (NTUA), Greece.
Reviewers:
(1) Saima Fazal, Huazhong University of Science and Technology, China.
(2) Heyuan Wang, Liaoning University of Technology, China.
Complete Peer review History: http://www.sciencedomain.org/review-history/17370

Original Research Article

Received 29th April 2016
Accepted 21st June 2016
Published 28th December 2016

ABSTRACT

Pollutants have grievous impacts on human lives and aquatic ecosystem. Reducing them in our environment is a global objective that demands cooperation from all, and the services of experts. In view of this, a hydrodynamic model of the spread of pollutants in a bifurcating river is presented to investigate the role of the flow dynamics of rivers in the dispersion of pollutants. The study is centred on the River Nun, Bayelsa, Nigeria where there are incidences of pollution. The flow model is governed by a set of nonlinear and coupled partial differential equations, solved by the methods similarity transformation and perturbation series expansions. Expressions for the temperature, concentration and velocity are obtained and analyzed graphically. The analyses show that the bifurcation angle, Reynolds number and thermal differentials increase the velocity of the flow. These results have attendant implications on the spread of pollutants in the River Nun. In particular, if the deposition of pollutants in a location of the river is stopped, the increase in velocity will enhance the spread of the existing pollutants through the infinite river, thus reducing their concentration at that location to an allowable level, safe for man and the aquatic ecosystem.

**Corresponding author: E-mail: wilsonia6011@gmail.com;*

Keywords: Bifurcation; magneto-hydrodynamics; perturbation; pollutants; River Nun.

1. INTRODUCTION

Streams and rivers are gifts of nature. They serve for drinking (in modern times, when treated), fishing, irrigation, transportation, power generation and the likes. Therefore, they are means of economic growth.

Societal economic activities impose negative effects on the aquatic systems, streams and rivers inclusive. Amongst these effects is pollution. The pollution may be caused by the introduction of chemicals, dumping of refuses, oil spillage which may be due to accidental discharge of petroleum products, and so on in certain locations of a river. The content of these materials are alkaline, acids, esters, heavy metals, and the likes. These substances increase the chemical composition of the water in such locations, and this becomes a problem when the concentration exceeds the maximum allowable value. At this level, the water becomes hazardous to aquatic lives and human body.

In this study, we shall consider the pollution situation in a bifurcating river, the River Nun in Bayelsa, Nigeria. The River Niger bifurcates into the Nun and Forcados Rivers about thirty-two kilometres downstream from Aboh, Delta State, Nigria. The Nun River is a stretch of fresh water flowing into the Gulf of Guinea, a wide inlet of the Atlantic Ocean at Akassa. It is about one hundred and sixty kilometres in length (Wikipedia, the free Encyclopedia [1]). In 1963 petroleum was discovered along river, about eighty- nine kilometres upstream. Similarly, in 1969, the Trans-Niger Pipeline that piped the oil from the river to Rumuekpe in River State, Nigeria was completed (Wikipedia, the free Encyclopedia [1]). Associated with the oil exploration and exploitation is the accidental discharge of oil into the river. The serious environmental damage caused by frequent oil spills and their impacts on human and marine lives made living in the polluted area a harrowing experience (Chinedu [2]). Furthermore, the Nun River bifurcates about five kilometres before the city of Yenagoa. It flows south- westernly behind Yenagoa. Along the banks of this section of the river are markets, homes, industries, plants, and so on. The solid and liquid wastes generated here are dumped into the river. Compounding these pollution sources is the direct channeling of untreated urban storm water and sewerage into the river (Ezekwe et al. [3]). From Ezekwe et al. [3] the water quality test reveals the following: p^H (6.3-7.3); turbidity level (65-66 FTU); dissolved materials (48-50 mg/l); oil and grease (7 mg/l); heavy metals levels, iron (>1915 mg/l), lead (>26 mg/l), cadmium (>12 mg/l), arsenic (6 mg/l). Chromium level is comparably low, while mercury is below a detectable limit. The presence of these key indicators affecting the chemical and biological quality of the river shows that this section of the fresh water suffers degradation from the negative effects of urbanization. A number of communities and fishing hamlets situated along this stretch of the Nun River such as Otuokpoti, Otuedu and Ewama that depend directly on the river for domestic uses, fishing and sport suffer from the effects of this pollution (Ezekwe et al. [3]).

Works exist in literature on the impacts of pollution on the environment and the inhabitants of the affected regions. Ezekwe et al. [3]; Odeyemi and Ogunseitan [4]; Mason [5]; Celestine [6]; Twumasi [7]; Chukuezi [8]; Ordinioha and Brisibe [9] have extensively discussed these. Nevertheless, on the effective evacuation of pollutants, and efforts made at reducing the occurrence of such incidences, not much is reported.

Reducing the pollution of the aquatic systems is one of the global objectives, achievable through appropriate management of water systems to maintain quality standard. Different methods have been employed for this. Some used software (see Tung et al. [10]), and others mathematical models (see Minsky [11]; Mannina [12]; Marusic and Moraru [13]; Marusic [14]). The use of mathematical models helps to predict the behaviour of the aquatic systems, and determine the results of the actions of the different processes in them.

More so, various models have been employed for studying the flow dynamics of streams and rivers. Some used the hydrologic model, which involves the use of spatial form of the continuity equation or water balance and flux relation expressing storage as a function of inflow and outflow; see Singh [15]. Some the hydraulic model, which is based on the use of St. Venant equations; see Hoey [16], and others the stochastic probability model, which involves the use of Monte Carlo method; see Hoey [2] and Singh [17]. Most recently, Pittaluga et al. [18] presented a 2-D hydrodynamic model for flood

simulation in a river. From the available models, there seems to be very few on the hydrodynamics of the streams and rivers. Therefore, we are motivated to make some impacts here. We shall present a hydrodynamic model of the spread of pollutants in a bifurcating river: the River Nun, Bayelsa, Nigeria.

There are a number of research reports on the hydrodynamic flow of fluid in both bifurcating and non-bifurcating systems. The concept of bifurcation (in sense that a flow system divides into two or more daughter channels) is seen in both natural and artificial settings. Therefore, it has applications in both science and engineering. Based on these, the attention of research workers have been drawn to it since the past decades. Pedley et al. [19] introduced the use of theoretical approach or mathematical tools in the study of branching flows. Sobey and Drazin [20] examined the stabilities and bifurcation of a two-dimensional channel flow using analytic, numerical and experimental methods, and observed that flow separation occurs near the wall, and that both separation and bifurcation do not occur together. Skalak et al. [21] investigated the three-dimensional symmetric one-to-two bifurcation using the analytic approach, and noticed that a flow separation or reversal occurs at the junction. Also, Liou et al. [22] studied the effect of bifurcation angles on the steady flow in a straight terminal aneurysm model with asymmetric outflow through the branches using the Laser-Doppler velocity and fluctuating intensity distribution. They observed that the size of the recirculation zones in the afferent vessel, the flow activity inside the aneurysm, and the shear stress acting on the aneurismal wall increase as the bifurcation angle increases. Drikakis and Leiber [23] conducted a numerical study on the effect of expansion ratio of the downstream: upstream on the flow, and was able to demonstrate the critical Reynolds number for asymmetric flow to occur. More so, Zhao [24] studied numerically and experimentally the steady aspiratory and expiratory flow in a three-dimensional airway system of single symmetric bifurcation. They showed that the flow results obtained from computational simulations are in good agreement with the experimental results, especially during expiration. Smith et al. [25] examined theoretically the behaviour of incompressible side-branching flow at high Reynolds number and compared it with that of direct numerical simulation at moderate Reynolds number, and observed that in the vicinity of the branch the flow adjusts to the imposed downstream pressure in the daughter through a jump in the flow properties across the daughter entrance. Furthermore, noticed that for large pressure drops in the daughter tube, the fluid is sucked in at high velocities from the mother and thereby provides a favourable upstream feedback. Pittaluga et al. [18] investigated the equilibrium configuration and stability of a channel bifurcation in braided rivers, and showed that an increase in bifurcation angle increases the transport velocity. Soulis [26] showed that changes in bifurcation angle alter the flow condition and changes the magnitude of the wall shear stress. Tadjar and Smith [27] investigated a three-dimensional one-to-two symmetrical flow in which the mother is straight and of circular cross-section, containing a fully developed incident motion, while the diverging daughters are straight and of semi-circular cross-section. Using the method of direct numerical simulation and slender modeling for a variety of Reynolds number and divergent angles, they observed that a flow separation or reversal occurs at the corners of the junction, and the inlet pressure increases as the bifurcation angle increases. Okuyade and Abbey [28] studied blood flow in bifurcating arteries using the method of regular perturbation, and noticed that an increase in bifurcation angle and Reynolds number increase the transport velocity factor.

The flow through porous media is prevalent in nature and artificial settings. Therefore, it is of principal interest in science and engineering. For this, Okuyade and Abbey [29] examined the fluid-mechanical aspect of the flow in bifurcating arteries, and observed that an increase in bifurcation angle and Reynolds number produces a commensurate increase in the wall shear stress. Berkermann et al. [30] examined free convective flow between a fluid and a porous layer in a rectangular enclosure. Rao and Sobha [31] investigated the flow in a rotating straight pipe and showed that the Nusselt number increases with increase in porosity. Furthermore, Avramenko and Kuznetsov [32] studied the flow in a curved porous channel with rectangular cross-section filled with a fluid saturated porous medium with the flow driven by a constant azimuthally pressure gradient using a generalized Fourier series method of solution, and found that the velocity profiles depend on the geometry of the channel and Darcy number.

Similarly, flow problems involving chemical reactions were considered. Shateyi et al. [33] studied a two-dimensional flow of an

incompressible viscous fluid through a non-porous channel with heat generation and chemical reaction by the methods of similarity transformation, homotopy analysis and numerical. They observed that an increase in the Reynolds number decreases the tangential velocity but increases the heat and mass transfer; the increase in the Eckert number and heat generation/absorption parameter increase the temperature; the increase in the chemical reaction parameter decreases the concentration profiles, and an increase in the Grashof number increases the flow velocity.

The study of the flow of fluid has also been extended to include the effect of magnetic field. Kaur et al. [34] considered the flow of viscous incompressible fluid embedded with small spherical particles in a non-conducting channel with hexagonal cross-section in the presence of a transverse magnetic field using the method of integral transformation, and noticed that the velocity of the fluid and particles decrease with increase in the intensity of magnetic field. Abdel-Malek and Helel [35] investigated the effect of magnetic field on the flow in a rectangular enclosure using perturbation technique, and reported that the imposed magnetic field diminished the wall shear stress. Asadolah et al. [36] examined the influence of magnetic field on the skin friction factor of a steady fully developed laminar flow through a pipe by experimental and finite difference numerical scheme. They observed that the pressure drop varies in proportion to the square of the magnetic field and the sine angle; the pressure is proportional to the flow rate, and the axial velocity asymptotically approaches its limit as the Hartmann number becomes large.

Works had been done on the magneto-hydrodynamic convective flow. Magneto-hydrodynamic convective heat and mass transfer in porous and non-porous media is of considerable interest in technical field due to its applications in industries, geothermal, high temperature plasma, liquid metal and MHD power generating systems. Chamkha and Quadri [37] examined the hydro-magnetic natural convection flow through a horizontal permeable cylinder, and obtained a numerical solution of the non-similar boundary layer problem. Malashetty et al. [38] examined the fully developed free convection two-fluid magneto-hydrodynamic flow in an inclined channel using the perturbation techniques, and found that the flow can be controlled effectively by suitable adjustment of the values for the ratios of heights, electrical conductivities and viscosities of the two fluids. Venkateswalu et al. [39] studied the free convection flow through a vertical porous channel in the presence of an applied magnetic field using the finite difference numerical approach, and noticed that the velocity decreases with the increase in the magnetic and porosity parameters throughout the region. Okuyade [40] investigated the effects of magnetic field and convective force on the flow in bifurcating porous fine capillaries, and found that magnetic field reduces the flow velocity, whereas the convective force increases it. Das et al. [41] considered the fully developed mixed convection flow in a vertical channel filled with nanofluids in the presence of a uniform transverse magnetic field using closed form solutions. They observed that magnetic field enhances the nanofluid velocity in the channel; the induced magnetic field vanishes in the central region of the channel. In addition, they noticed that the critical Raleigh number at the onset of the instability of the flow is strongly dependent on the volume fraction of nanoparticles and the magnetic field. More so, Okuyade and Abbey [42] examined blood flow in bifurcating arteries analytically, and observed that an increase in heat exchange parameter and Grashof number increase the velocity, concentration and Nusselt number of the flow, while an increase in the heat exchange parameter increases the Sherwood number.

This paper examines the dispersion of pollutants in a bifurcating stream using the hydrodynamic approach. We shall investigate the effects of bifurcation angle, Reynolds number, and thermal parameters on the spread and evacuation of pollutants from the affected locations of the stream.

This paper is organized in the following format: section 2 is the methodology; section 3 holds the results and discussion, and section 4 gives the conclusions.

2. METHODOLOGY

The river is approximately rectangular in form and has a planar surface. We assume that flow is symmetrical in the z-axis; the fluid is chemically reacting and of a homogeneous first order type (a reaction which is directly proportional to the concentration); the porous medium is non-homogeneous therefore its permeability is anisotropic. Additionally, we assume that the fluid has constant properties except that the density

varies with the temperature and concentration, which are considered only in the force term; the viscosity of the fluid is a function of temperature and magnetic field, and the flow field is such that there are pressure, temperature and concentration gradients. If (u, v) are respectively the velocity components of the fluid in the mutually orthogonal (x, y) axes, the mathematical equations of mass balance or continuity, momentum, energy and diffusion governing the flow in the presence of bifurcation, and considering the Boussinesq and Swell's free flow in the dimensionless form are:

$$\frac{\partial u}{\partial x}+\frac{\partial v}{\partial y}=0 \tag{1}$$

$$\mathrm{Re}\left(u\frac{\partial u}{\partial x}+v\frac{\partial u}{\partial y}\right)=-\frac{\partial p}{\partial x}+\left(\frac{\partial^2 u}{\partial x^2}+\frac{\partial^2 u}{\partial y^2}\right) \tag{2}$$
$$+Gr\Theta+Gc\Phi-\chi^2 u-M^2 u$$

$$\mathrm{Re}\left(u\frac{\partial v}{\partial x}+v\frac{\partial v}{\partial y}\right)=-\frac{\partial p}{\partial y}+\left(\frac{\partial^2 v}{\partial x^2}+\frac{\partial^2 v}{\partial y^2}\right) \tag{3}$$

$$\mathrm{Re}\,\mathrm{Pr}\left(u\frac{\partial \Theta}{dx}+v\frac{\partial \Theta}{\partial y}\right)=\left(\frac{\partial^2 \Theta}{dx^2}+\frac{\partial^2 \Theta}{\partial y^2}\right)+N^2\Theta \tag{4}$$

$$\mathrm{Re}\,Sc\left(u\frac{\partial \Phi}{dx}+v\frac{\partial \Phi}{\partial y}\right)=\left(\frac{\partial^2 \Phi}{dx^2}+\frac{\partial^2 \Phi}{\partial y^2}\right)+\delta_1^2\Phi \tag{5}$$

The problem examines the dynamics of a bifurcating river flowing from a point $x=-\infty$ through a shore at $x=x_o$ and continues towards $x=+\infty$, as seen in Fig. 1. The model shows that the channel is assumed symmetrical and divided into two regions: the upstream (or mother) region $x<x_o$ and downstream (or daughter) region $x>x_o$, where x_o is the bifurcation or the nodal point, which is assumed the origin such that the river boundaries become $y=\pm d$ for the upstream region and $y=\alpha x$ for the downstream region. Due to geometrical transition between the mother and daughter channels, the problem of wall curvature effect is bound to occur. To fix up this, a very simple transition wherein the width of the daughter channel is made equal to half that of the mother channel i.e. $\pm d$ such that the variation of the bifurcation angle is straightforwardly used (see [27]). Furthermore, if the width of the stream ($2d$) is far less than its length (l_o) before the point of bifurcation such that the ratio of $\frac{2d}{l_o}=\Re<<1$, (where $\Re$ is the aspect ratio), the flow is laminar and Poiseuille (see [43]). d is assumed to be non-dimensionally equal to one (see [27]). Similarly, at the entry region of the mother channel, the flow velocity is given as $u=U_o\left(1-y^2\right)$, where U_o is the characteristic velocity, which is taken to be maximum at the centre and zero at the wall (see [13]). Based on the fore going, the boundary conditions are:

$$u=1,\ v=0,\ \Theta=1,\ \Phi=1 \text{ at } y=0 \tag{6}$$

$$u=0,\ v=0,\ \Theta=\Theta_w,\ \Phi=\Phi_w \text{ at } y=1 \tag{7}$$

for the upstream channel

$$u=0,\ v=0,\ \Theta=0,\ \Phi=0 \text{ at } y=0 \tag{8}$$

$$u=0,\ v=0,\ \Theta=\gamma_1\Theta_w,\ \Phi=\gamma_2\Phi_w,\ \gamma_1<1,\ \gamma_2<1 \text{ at } y=\alpha x \tag{9}$$

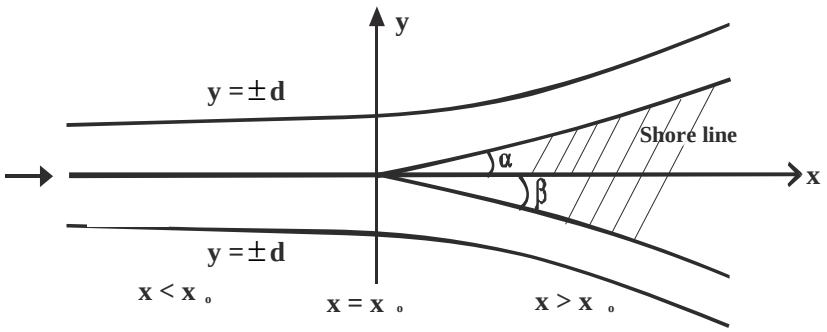

Fig. 1. A physical model illustrating the concept of symmetrical bifurcation in a river (α and β are the bifurcation angles and are equal)

for the downstream channel

where

$$x=\frac{x'}{l_c},\ y=\frac{y'}{l_c},\ u=\frac{u'}{U_o},\ v=\frac{v'}{U_o},\ p=\frac{p'}{p_\infty},$$
$$\rho=\rho' U_o^2,\ \Theta=\frac{T'-T_\infty}{T_w-T_\infty},\ \Phi=\frac{C'-C_\infty}{C_w-C_\infty},$$
$$\upsilon=\frac{\mu}{\rho},\ \mathrm{Re}=\frac{\rho U_o l_c}{\mu},\quad Gr=\frac{\rho g\beta_t(T_w-T_\infty)l_c^2}{\mu U_o},$$
$$Gc=\frac{\rho g\beta_c(C_w-C_\infty)l_c^2}{\mu U_o},\ \chi^2=\frac{l_c^2}{\kappa},\quad \delta_1^2=\frac{k_r^2 l_c^2}{D}$$
$$,\ M^2=\frac{\sigma_e B_o^2 l_c^2}{\rho\mu\mu_m},\ N^2=\frac{\mu C_p l_c^2}{k_o},\ Sc=\frac{\mu}{\rho D}$$

are the dimensionless variables; β_t and β_c are the volumetric expansion coefficient for temperature and concentration respectively; p_∞ is the ambient/equilibrium pressure; C_∞ is the concentration at equilibrium. T_∞ is the temperature at equilibrium; κ is the permeability parameter of the porous medium; B_o^2 is the applied uniform magnetic field strength due the nature of the fluid; σ_e is the electrical conductivity of the fluid. k_o is the thermal conductivity; C_p is the specific heat capacity at constant pressure; Q is the heat absorption coefficient; D is the diffusion coefficient. k_r^2 is the rate of chemical reaction of the fluid, which is homogeneous and of order one; C' is the concentration (quantity of material being transported); g is the gravitational field vector. p is the pressure; T' is the fluid temperature; ρ is the density of the fluid; μ is the viscosity of the fluid. μ_m is the magnetic permeability of the fluid; υ is the kinematic viscosity; l_c is the scale length. C_w is the constant wall temperature is maintained; T_w is the constant wall concentration at which the channel is maintained; Re is the Reynolds number. Gr is the Grashof number due to temperature difference; Gc is the Grashof number due to concentration difference; χ^2 is the local Darcy number. M^2 is the Hartmann's number; Pr is the Prandtl number; Sc is the Schmidt number. δ_1^2 is the rate of chemical reaction, and N^2 is the heat exchange parameter.

Introducing the similarity transformation solutions:

$$\Psi=(U_o\upsilon x)^{1/2} f(\eta),\ \eta=\left(\frac{U_o}{\upsilon x}\right)^{1/2} y \qquad (10)$$

with the velocity components represented

$$u=\frac{\partial\Psi}{\partial y},\ v=-\frac{\partial\Psi}{\partial x} \qquad (11)$$

into equations (1) - (9), we have

$$f''=0 \qquad (12)$$

$$f'''+f''-M_1^2 f'+\mathrm{Re}(f'f''+ff'')=-Gr\,\Theta-Gc\,\Phi \qquad (13)$$

$$\Theta''+\Theta'+\mathrm{Re}\,\mathrm{Pr}(-f'\Theta'+f\Theta')+N^2\Theta=0 \qquad (14)$$

where $M_1^2=M^2+\chi^2$, f is the similarity velocity, and η is the independent similarity variable

with the boundary conditions:

$$f=1,\ f'=0,\Theta=1,\Phi=1 \quad \text{at } \eta=0 \qquad (15)$$

$$f'=0,\ f=0,\ \Theta=\Theta_w,\ \Phi=\Phi_w \quad \text{at } \eta=1 \qquad (16)$$

for the upstream channel

$$f=0,\ f'=0,\Theta=0,\Phi=0 \quad \text{at } \eta=0 \qquad (17)$$

$$f'=0,\ f=0,\Theta=\gamma_1\Theta_w,\Phi=\gamma_2\Phi_w,$$
$$\gamma_1<1,\gamma_2<1 \quad \text{at } \eta=ax \qquad (18)$$

for the downstream channel

Equations (12) - (14) show that the similarity equations are coupled and highly non-linear. Therefore, to linearize and make them tractable, we seek for regular perturbation series solutions of the form

$$h(x,y)=h_o(x,y)+\xi h_1(x,y)+\ldots \qquad (19)$$

where $\xi = \frac{1}{\mathrm{Re}} << 1$ is the perturbing parameter. The choice of this parameter is because, almost at the point of bifurcation, due to a change in the geometrical configuration, the inertial force rises and the momentum increases. The increase in the momentum is associated with a drastic increase in the Reynolds number. Since the Reynolds number at the nodal point is very high, its reciprocal will be very small. In this regard, equations (12) - (14) become,

for the zeroth order:

$$f_o'' = 0 \tag{20}$$

$$f_o''' + f_o'' - M_1^{\,2} f_o' = -Gr\Theta_o - Gc\Phi_o \tag{21}$$

$$\Theta''_o + \Theta'_o + N^2\Theta_o = 0 \tag{22}$$

$$\Phi_o'' + \Phi_o' + \delta^2{}_1\Phi_o = 0 \tag{23}$$

with the boundary conditions

$$f_o = 1,\ f_o^{'} = 0,\ f_o^{''} = 0, \Theta_o = 1, \Phi_o = 1 \quad \text{at} \quad \eta = 0 \tag{24}$$

$$f_o = 0,\ f_o^{'} = 0,\ f_o^{''} = 0, \Theta_o = 0, \Phi_o = 0 \ \text{at} \ \eta = 1 \tag{25}$$

and for the first order:

$$f_{1.}'' = 0 \tag{26}$$

$$f_1''' + f_1'' - M_1^{\,2} f_1^{'} = f_o' f_o'' - f_o f_o'' - Gr\Theta_1 - Gc\Phi_1 \tag{27}$$

$$\Theta_1'' + \Theta_1' + N^2\Theta_1 = \mathrm{Pr}(f_o'\Theta'_o - f_o\Theta'_o) \tag{28}$$

$$\Phi_1'' + \Phi_1' + \delta_1^{\,2}\Phi_1 = Sc(f_o'\Phi_o' - f_o\Phi_o') \tag{29}$$

with the boundary conditions

$$f_1 = 0,\ f_1^{'} = 0, \Theta_1 = 0, \Phi_1 = 0 \quad \text{at} \quad \eta = 0 \tag{30}$$

$$f_1 = 0,\ f_1^{'} = 0, \Theta_1 = \gamma_1\Theta_w, \Phi_1 = \gamma_2\Phi_w, \quad \gamma_1 < 1, \gamma_2 < 1 \quad \text{at} \quad \eta = ax \tag{31}$$

The zeroth order equations describe the flow in the upstream channel, while the first order equations describe the flow in the downstream channels. The zeroth order terms in the first order equations indicate the influence of the upstream on the downstream flow.

The solutions to equations (20) - (25) and (26) - (31) are:

$$\Theta_o(\eta) = \frac{\Theta_w e^{\frac{1}{2}(1-\eta)} \sinh\mu_1\eta}{\sinh\mu_1} + \frac{e^{-\frac{1}{2}(1-\eta)} \sinh\mu_1(1-\eta)}{\sinh\mu_1} \tag{32}$$

$$\Phi_o(\eta) = \frac{\Phi_w e^{\frac{1}{2}(1-\eta)} \sinh\mu_2\eta}{\sinh\mu_2} + \frac{e^{-\frac{1}{2}(1-\eta)} \sinh\mu_2(1-\eta)}{\sinh\mu_2} \tag{33}$$

$$f_o(\eta) = \frac{\left(f_{o(p)}(0)e^{-(\mu 3+\eta/2)} \sinh\mu_3\eta\right)}{\sinh\mu_3} + \frac{\left(f_{o(p)}(1)e^{-1/2(1-\eta)} \sinh\mu_3\eta\right)}{\sinh\mu_3} - f_{o(p)}(0)e^{-(\mu_3+\eta/2)} + f_{o(p)}(\eta) \tag{34}$$

and

$$\Theta_1(\eta) = \frac{\gamma_1\Theta_w e^{\frac{1}{2}(\alpha x-\eta)} \sinh\mu_1\eta}{\sinh(\mu_1\alpha x)} - \frac{\Theta_{1(p)}(\alpha x)e^{-\frac{1}{2}(\alpha x-\eta)} \sinh\mu_1\eta}{\sinh(\mu_1\alpha x)} + \frac{\Theta_{1(p)}(0)e^{-(\mu\alpha x+\eta/2)} \sinh\mu_1\eta}{\sinh(\mu_1\alpha x)} - \Theta_{1(p)}(0)e^{-(\alpha x-(\mu_1+1/2)\eta\ )} + \Theta_{1(p)}(\eta) \tag{35}$$

$$\Phi_1(\eta)=\frac{\gamma_2\Phi_w e^{\frac{1}{2}(\alpha x-\eta)}\sinh\mu_2\eta}{\sinh(\mu_2\alpha x)}+\frac{\Phi_{1(p)}(\alpha x)e^{-\frac{1}{2}(\alpha x-\eta)}\sinh\mu_2\eta}{\sinh(\mu_2\alpha x)}$$
$$+\frac{\Phi_{1(p)}(0)e^{-(\mu\alpha x+\eta/2)}\sinh\mu_2\eta}{\sinh(\mu_2\alpha x)}-\Phi_{1(p)}(0)e^{-(\alpha x-(\mu_2+1/2)\eta\ )}+\Phi_{1(p)}(\eta) \quad (36)$$

$$f_1(\eta)=\frac{f_{1(p)}(0)e^{-(\mu_3\alpha x+\eta/2)}\sinh\mu_3\eta}{\sinh\mu_3\alpha x}+\frac{f_{1(p)}(\alpha x)e^{1/2(\alpha x-\eta)}\sinh\mu_3\eta}{\sinh(\mu_3\alpha x)}$$
$$-f_{1(p)}(0)e^{(\alpha x-(\mu_{3+1/2})\eta)}+f_{1(p)}(\eta) \quad (37)$$

where $f_{o(p)}(\eta)$, $\Theta_{1(p)}(\eta)$, $\Phi_{1(p)}(\eta)$, $f_{1(p)}(\eta)$ are expanded in the appendices

3. RESULTS AND DISCUSSION

We consider the effects of some geometrical and dynamical parameters such as bifurcation angle, Reynolds number, environmental thermal differentials and magnetic field on the spread of pollutants in a bifurcating stream. To this end, Figs. 2–13 which are obtained using Maple 12 computational software show the computational results for the temperature and velocity when the bifurcation angle, Reynolds number, heat exchange parameter, Grashof numbers and magnetic field are varied. For physically realistic constant values of Pr =0.71; γ_1 = 0.6; γ_2 =0.6; γ =0.7; Φ_w = 2.0; Θ_w =2.0; $\delta_1^2=0.2$; χ^2 =0.2, and varying values of

α=5, 10, 15, 20;
Re=10000, 1000, 100, 10, 5;
N^2 = 0.01, 0.1, 0.5, 1.0;
Gr= 0.1, 0.5, 1.0, 5.0;
M^2 = 0.01, 0.1, 0.5, 1.0;

the profiles show that the

* Increase in bifurcation angle increases the temperature and velocity,
* Increase in the Reynolds number increases the temperature and velocity,
* Increase in the Grashof numbers increases the temperature and velocity,
* Increase in the heat exchange parameter increases the temperature;
* Increase in the magnetic field parameter reduces the velocity, and makes the motion oscillatory/fluctuating.

For the bifurcation angle, an increase in the angle of bifurcation narrows down the width of the river. This in turn increases the inlet pressure in the downstream region. Consequently, the pressure increases the velocity flow structure, as seen in Figs. 4 and 5. These results are in complete agreement with [18,25,27,28,32]. Moreover, since velocity is a function of energy its increase leads to an increase in the energy of the system; see Figs. 2 and 3.

Next, we consider the effects of the Reynolds number. The flow in the upstream region is laminar and Poiseuille; therefore, its Reynolds number is moderate. However, almost at the point of bifurcation or the entry point of the downstream region, the flow exhibits some oscillatory behaviour in the upstream region due to a change in the geometrical configuration. At this point, the inertial force rises, leading to a drastic increase in the Reynolds number, indicating a sort of turbulent flow. As the Reynolds number increases, the velocity in turn increases, thus causing the water to rush into the downstream region with a great force; see in Figs. 6 and 7. These results agree with [29]. It is interesting to notice that the flow regains its laminar nature some distance away from the entry point.

In addition, we look at the effects of the heat exchange parameter. As the environmental temperature increases due to increasing radiation from the sun heat is absorbed into the stream. The rise in the heat level energizes the water particles such that their kinetic energy increases (see Fig. 8). In another development, the rise in the kinetic energy tends to increase the velocity of the fluid particles. This is in consonance with [43].

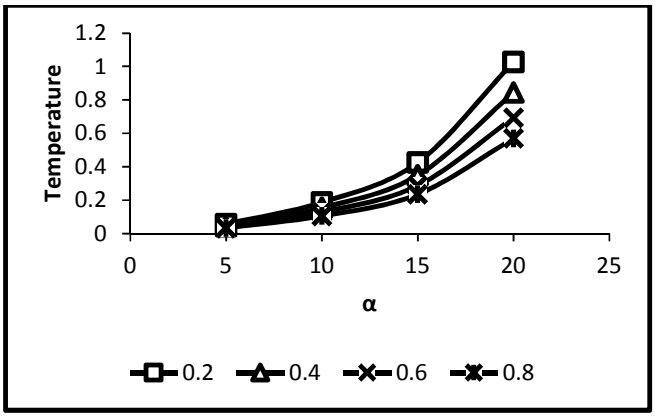

Fig. 2. Temperature profiles for various bifurcation angles (α) in the daughter channel

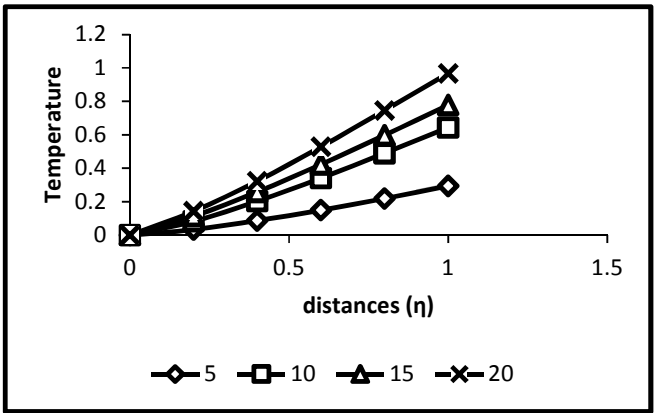

Fig. 3. Temperature-bifurcation angle (α) profiles at various distances (η) in the daughter channel

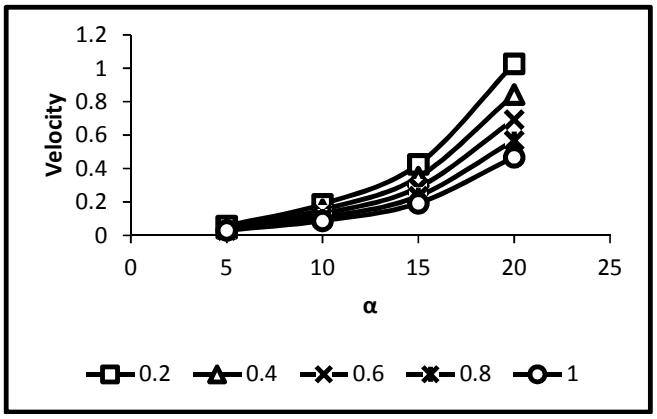

Fig. 4. Velocity profiles for various bifurcation angles (α) in the daughter channel

On the Grashof number, the increase in the thermal gradient arising from the increase in the environmental temperature in the presence of gravity generates convective current, otherwise called the Grashof number. This reduces the viscosity and causes the fluid particles to gain more energy to become buoyant. The convective/buoyancy force serves as a lifting force to the fluid particles, and this in turn increases the velocity; see Figs. 9 and 10. These findings are in agreement with [34.41,43].

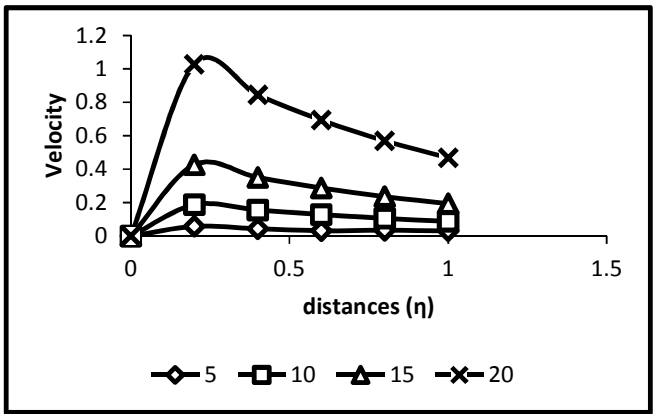

Fig. 5. Velocity -bifurcation angle (α) profiles at various distance (η) in the daughter channel

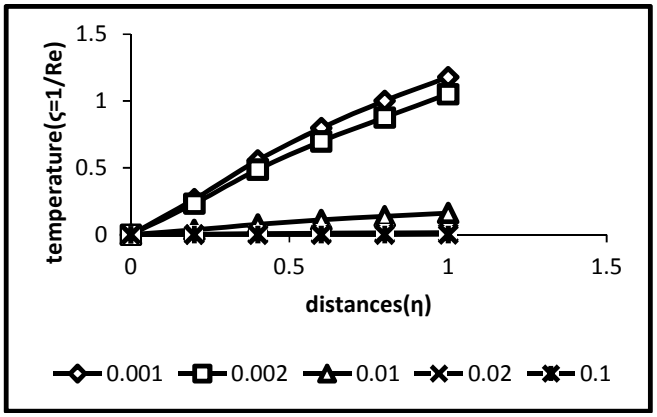

Fig. 6. Temperature –Reynolds number (Re) profiles at various distances (η) in the daughter channel

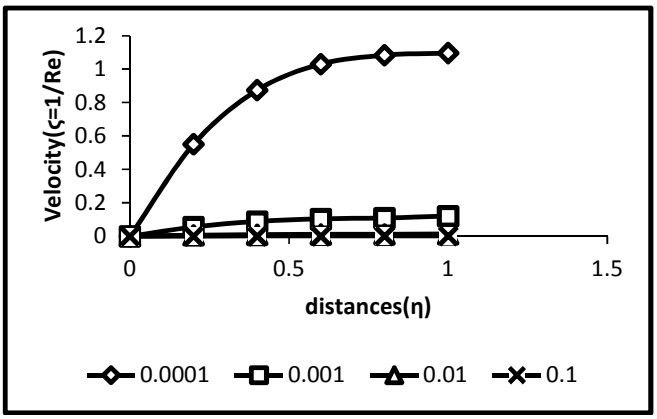

Fig. 7. Velocity-Reynolds number (Re) profiles at various distances (η) in the daughter channel

For the magnetic field effects, the source rocks of the river in the mountain may be made of metallic oxides and salts. These dissolve in the water to make it alkaline or saline. With this, the water becomes electrolytic, and therefore, exists as charges. The action of the earth magnetic field on the charges produces a mechanical force, the Lorentz force, which gives the flow a new orientation. In particular, the Lorentz force has a freezing impact on the velocity flow structure, thus accounting for the observation in Fig. 11.

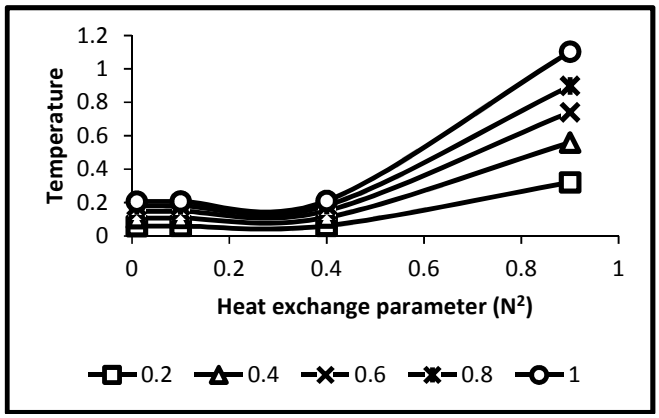

Fig. 8. Temperature profiles for various heat exchange parameter (N^2) in the daughter channel

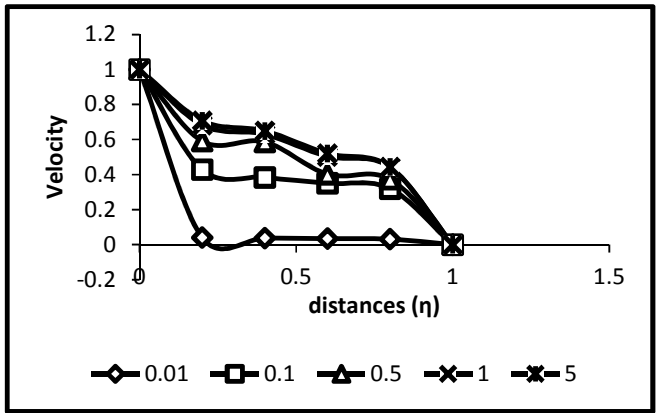

Fig. 9. Velocity-Grashof number (Gr/Gc) profiles at various distances (η) in the mother channel.

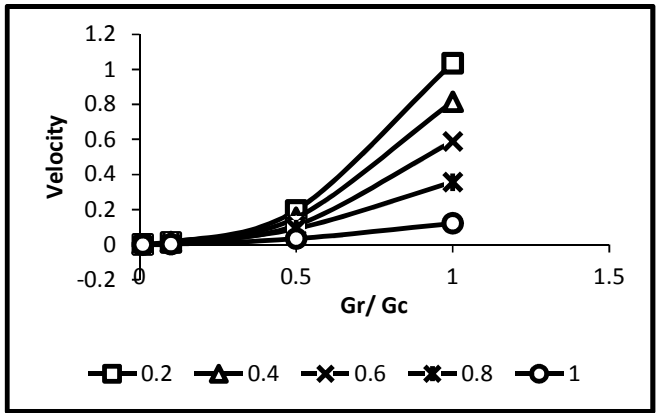

Fig. 10. Velocity profiles for various Grashof numbers (Gr/Gc) in the daughter channel

This result is in alignment with those of [35], [37], [40] and [41]

Similarly, the oscillatory/fluctuating motion manifested in the form of back-and-forth movement of the water, as seen in Figs. 12 and 13, possibly, in addition, may be due to the internal waves developed in the water in the flow process, or may be caused by the interaction between the pressure forces and the gravity forces. The oscillatory/fluctuating motion of the water leads to loss of energy for the flow in the axial direction.

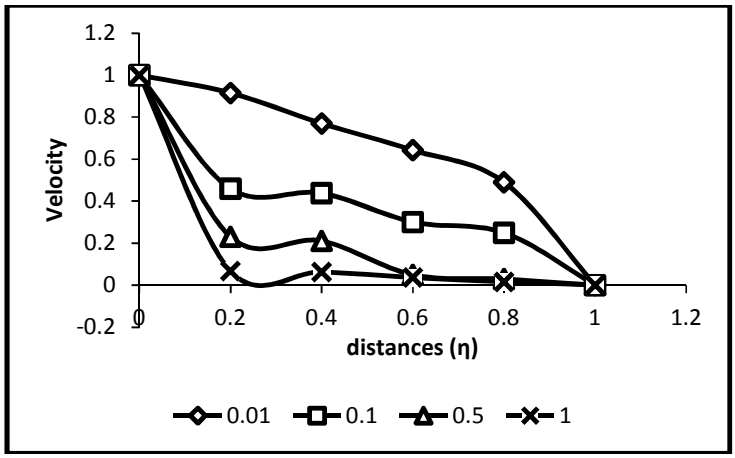

Fig. 11. Velocity-magnetic field parameter (M^2) profiles at various distances (η) in the mother channel

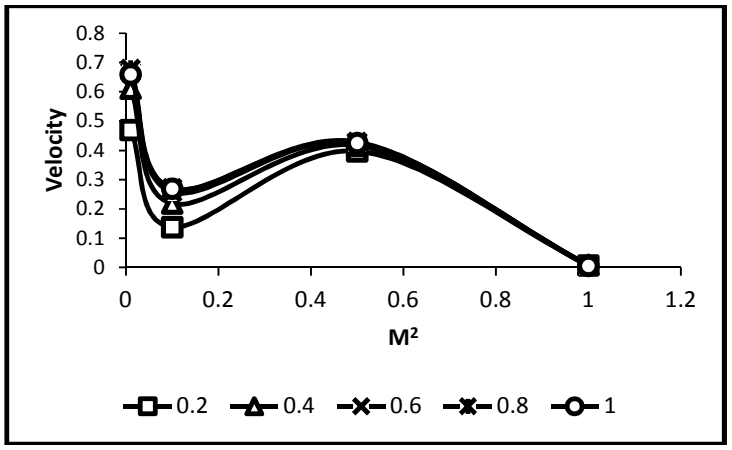

Fig. 12. Velocity profiles for various magnetic field parameter (M^2) in the daughter channel

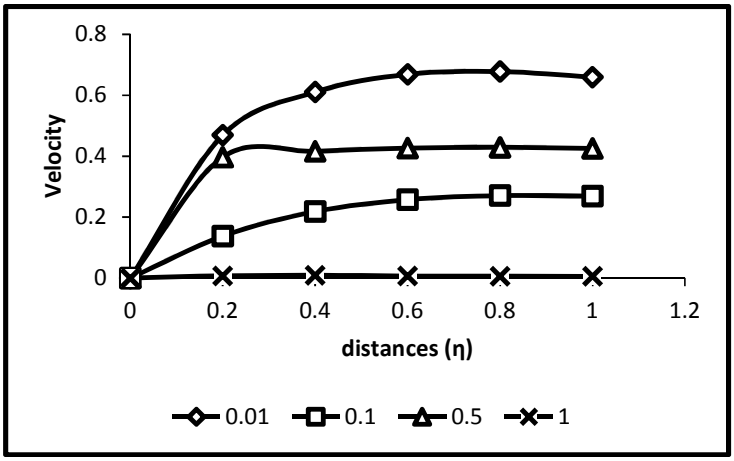

Fig. 13. Velocity-magnetic field parameter (M^2) profiles at various distances (η) in the daughter channel

Pollutants in a river are found concentrated at particular locations. Transporting them through an infinite river flowing towards a standing water body reduces their concentration, possibly, to an allowable quality standard. Therefore, the increase and decrease in temperature and velocity coupled with the oscillatory/fluctuating motion have attendant implications on the spread and control of pollutants in a flowing river. In particular, the increase in velocity enhances their spread, thus bringing their concentration at such location to an allowable level, safe for the aquatic ecosystem and human body. On the contrary, the decrease in the velocity and the oscillatory/fluctuating motion inhibit their spread.

4. CONCLUSION

The problem of reducing pollution in our environment is of global concern. It is complex, therefore, demands the involvement of experts. Based on this, a hydrodynamic model of the spread of pollutants in a bifurcating river is presented with the aimed of investigating the role of the flow dynamics of the river on the evacuation of pollutants. The study is centred on the River Nun where there are incidences of pollution. In this study, the effects of some hydrodynamic and geometrical parameters are investigated. The analyses of the results show that the

* Increase in bifurcation angle increases the temperature and velocity;
* Increase in Reynolds number increases the temperature and velocity;
* Increase in Grashof numbers increases the temperature and velocity;
* Increase in heat exchange parameter increases the temperature;
* Increase in magnetic field decreases the velocity, and makes the motion oscillatory/fluctuating.

The increase and decrease in these flow variables coupled with the oscillatory/fluctuating motion have significant implications on the spread of pollutants in rivers. The increase in the flow velocity enhances the spread; while the decrease coupled with the oscillatory /fluctuating motion inhibit it. In particular, if the deposition of pollutants in a location of the river is stopped, the increase in velocity will enhance the spread of the existing pollutants through the infinite river, thus reducing their concentration at that location to an allowable level, safe for man and the aquatic ecosystem. This study has increased our understanding of the natural dispersion of pollutants in flowing streams and rivers.

COMPETING INTERESTS

Authors have declared that no competing interests exist.

REFERENCES

1. Wikipedia, the free Encyclopedia. The Nun River.
2. Chinedu OI. Oil spill disaster in Nigeria-Bonga field oil spill disaster. AWE International Magazine; 2012.
   Available:www.aweimagazine
3. Ezekwe IC, Odu MN, Gasa A. Pollution from non-oil sources in the River Nun downstream of Yenagoa Town. Estud Biologia. 2014;36(86):12-23.
4. Odeyemi O, Ogunseitan OA. Petroleum industry and its pollution potential in Nigeria oil and petroleum pollution. Elsevier Applied Science Publishers Ltd, England.1985;2:223-9.
5. Mason CF. Biology of fresh water pollution. England: Essex University; 2002.
6. Celestine A. Hydrocarbon exploration, environmental degradation and poverty: The Niger Delta experience. Diffusion Pollution Conference, Dublin; 2003.
7. Twumasi Y, Merem E. GIS and remote sensing application in the assessment of change within a coastal environment in the Niger Delta region of Nigeria. International J Environmental Research and Public Health. 2006;3(1):98-106.
8. Chukuezi C. Oil exploration and human security in Nigeria: A challenge to sustainable development. Federal Ministry of Environment, Abuja, Nigeria; Nigeria Conservation Foundation, Lagos; Niger Delta Damage Assessment and Restriction Project; 2006.
9. Ordinioha B, Brisibe S. The human health implication of crude oil spills in the Niger Delta, Nigeria: An interpretation of published studies. Nigeria Medical J. 2013; 54(1):10-6.
10. Mannina G. Uncertainty assessment of a water quality model for the Ephemeral River using glue analysis. J Environmental Engineering. 2011;137(3):177-186.
11. Minsky M. Models, minds machines. Proceeding IFIP. 1965;45-9.

12. Mannina G. Uncertainty assessment of a water quality model for the Ephemeral River using Glue analysis. J Environmental Engineering. 2011;137(3):177-186.
13. Marusic G, Moraro V. Mathematical modeling of pollutants transport for a sector of the Prut River. Proceeding of the 3rd International Conference on Mathematical Modeling, Optimization and Information Technology. Academy of Transport, Information and Communication of Moldova, Chisnau. 2012;86-98.
14. Marusic Galino. A study on the mathematical modeling of water quality in river-type aquatic system. WSEAS Transactions on Fluid Mechanics. 2013; 80–9.
15. Singh VP. Hydrologic systems: Rainfall - run-off modeling, Prentice House: Englewood Cliffs, New Jersey. 1988;1.
16. Hoey T. Temporal variations in bed load transport rate and sediment storage in gravel-bed rivers, Prog. Physical Geography. 1992;16(3):319–338.
17. Singh VP. Kinematic wave modeling in water resources: Surface water hydrology. John Wiley and Sons, New York; 1996.
18. Pittaluga MB, Repetto R, Tubino M. Channel bifurcation in braided rivers: Equilibrium configuration and stability. Water Resources Research. 2003;39(3): 1046–57.
19. Pedley TJ, Schroter RC, Sudlow MF. The prediction of pressure drop and variation of resistance within the human bronchial airways. Resp. Physiology. 1970;9:387–405.
20. Sobey J, Philip Drazin G. Bifurcating two-dimensional flow. J Fluid Mechanics. 1986; 171:263-87.
21. Skalak Richard, Skalak Thomas, Nihat Ozkaya. Biofluid Mechanics. Rev. Fluid Mechanics. 1989;21:167–204.
22. Liou TM, Change TW, Change WC. Effects of bifurcation angle on the steady flow structure in model saccular aneurysms. Experiments in Fluids. 1993;289–295.
23. Drikakis D. Bifurcation phenomena in an incompressible sudden expansion flow. Phys. Fluids. 1997;9:76–86.
24. Zhao Z, Leiber BB. Steady expiratory flow in a model symmetric bifurcation. J Biomech Eng. 1994;116:318–23.
25. Smith FT, Ovenden NC, Frank P, Doorly DJ. What happens to pressure when a fluid enters a side branch. J Fluid Mechanics. 2003;479:231–58.
26. Soulis. J Biomech. 2004;39:742–49.
27. Tadjar M, Smith FT. Direct simulation and modeling of a 3- dimensional bifurcating tube flow. J Fluid Mechanics. 2004;519:1-32.
28. Okuyade WIA, Abbey TM. Analytic study of blood flow in bifurcating arteries, part 1- effects of bifurcating angle and magnetic field. International Organization of Scientific Research J Mathematics; 2015. I.D: G54040 - (in press)
29. Okuyade WIA, Abbey TM. Analytic study of blood flow in bifurcating arteries, part 3- on wall shear stress. International Organization of Scientific Research J Mathematics; 2015.
I.D: G54041- (in press)
30. Beckermann C, Ramdhyani S, Viskanta R. Natural convection flow and heat transfer between a fluid layer and a porous layer inside a rectangular enclosure. J Heat Transfer. 1987;109:363–370.
31. Rao Ramana VV, Sobha VV. Heat transfer of a saturated porous flow in a rotating straight pipe. Proceeding of the Tenth National Heat and Mass Transfer Conference, Madurai Kamoraj University, Madurai. 1987;13.
32. Avramenko AA, Kuznetsov AV. Flow in a curved porous channel with rectangular cross-section. J Porous Media. 2008;241-48.
DOI: 10.1615/JporMedia.v.11.i3.20
33. Shateyi S, Motsa SS, Sibanda P. Homotopy analysis of heat and mass transfer boundary layer flow through a non-porous channel with chemical reaction and heat generation. The Canadian J Chemical Engineering. 2010;88:975-982.
34. Kaur JP, Singh GD, Sharma RG. Unsteady porous channel flow of a conducting fluid with suspended particles. Defense Science. 1988;38(1):13-20.
35. Abdel-Malek MB, Helal MM. Similarity solutions for magneto-force unsteady free convective laminar boundary–layer flow. J Comput. App. Maths. 2008;218:202–14.
36. Asadolah, Malekzadeh, Amir Heydarinasab, Bahram Dabir. Magnetic field effect on fluid flow characteristic in a

pipe for laminar flow. J Mechanical Sci. and Tech. 2011;25:333-39.
37. Chamkha AJ, Quadri MMA. J Heat Transfer. 2001;A40:387–401.
38. Malashetty MS, Umvati JS, Prathap Kumar J. Convective MHD flow heat transfer in an inclined channel. Heat and Mass Transfer. 2001;37:259-64.
39. Venkateswalu S, Suryanarayama Rao KV, Rambupal Reddy B. Finite difference analysis on convective heat transfer flow through porous medium in a vertical channel with magnetic field. Indian Journal of Applied Maths and Mechanics. 2011; 7(7):74–94.
40. Okuyade WIA. MHD blood flow in bifurcating porous fine capillaries. African J Science Research. 2015;4(4):56-59.
41. Das S, Jana RN, Makinde OD. Mixed convection magneto-hydrodynamic flow in a channel filled with nanofluids. Elsevier J Engineering Science and Technology. 2015;244-255.
DOI:http://dx.doi.org/10.1016/j.jestch 2014.12009
42. Okuyade WIA, Abbey TM. Analytic study of blood flow in bifurcating arteries, part 2- effects of environmental temperature differentials. International Organization of Scientific Research J Mechanical Engineering; 2015.
I.D: G54083 - (in press)
43. Bestman AR. Global models for the biomechanics of green plants, part 1. International J Energy Research 1991;16: 677–84.

APPENDICES

$$+\frac{n_3}{n_3\left(n_3^2-n_2n_3\right)}\left(\frac{GrAe^{\lambda_1\eta}}{\left(\lambda_1-n_2\right)}+\frac{GrBe^{\lambda_2\eta}}{\left(\lambda_2-n_2\right)}+\frac{GrCe^{m_1\eta}}{\left(m_1-n_2\right)}+\frac{GrDe^{m_2\eta}}{\left(m_2-n_2\right)}\right)$$

$$-\frac{1}{n_3\left(n_3^2-n_2n_3\right)}\left(\frac{GrAe^{\lambda_1\eta}}{\left(\lambda_1-n_3\right)}+\frac{GrBe^{\lambda_2\eta}}{\left(\lambda_2-n_3\right)}+\frac{GrCe^{m_1\eta}}{\left(m_1-n_3\right)}+\frac{GrDe^{m_2\eta}}{\left(m_2-n_3\right)}\right)$$

$$\lambda_1=-\frac{1}{2}+\frac{\sqrt{1-4N^2}}{2},\ \lambda_2=-\frac{1}{2}-\frac{\sqrt{1-4N^2}}{2}$$

$$\lambda_1=-\frac{1}{2}+\mu_1,\lambda_2=-\frac{1}{2}-\mu_1,\mu_1=\frac{\sqrt{1-4N^2}}{2}$$

$$m_1=-\frac{1}{2}+\mu_2,m_2=-\frac{1}{2}-\mu_2,\mu_2=\frac{\sqrt{1-4\delta_1^2}}{2}$$

$$n_2=-\frac{1}{2}+\mu_3,n_3=-\frac{1}{2}-\mu_3,\mu_3=\frac{\sqrt{1-4M^2}}{2}$$

$$A=\frac{\Theta_w e^{1/2}-e^{\mu_1}}{\sinh\mu_1},B=\frac{e^{\mu_1}-\Theta_w e^{1/2}}{\sinh\ \mu_1}\ C=\frac{\Phi_w e^{1/2}-e^{\mu_2}}{\sinh\mu_2},D=\frac{e^{\mu_2}-\Phi_w e^{1/2}}{\sinh\mu_2}$$

$$\Theta_{1(p)}(\eta)=\frac{\Pr}{(\lambda_2-\lambda_1)}[\ \ \lambda_1FAe^{(\lambda_1+n_2)\eta}+\lambda_1GAe^{(\lambda_1+n_3)\eta}$$

$$-\left(\frac{n_3}{n_2\left(n_3^2-n_2n_3\right)}-\frac{1}{\left(n_3^2-n_2n_3\right)}\ \right)\left(\begin{array}{l}GrA^2e^{2\lambda_1\eta}+\frac{\lambda_1GrABe^{(\lambda_1+\lambda_2)\eta}}{\lambda_2}+\frac{\lambda_1GcACe^{(\lambda_1+m_1)\eta}}{m_1}\\+\frac{\lambda_1GcADe^{(\lambda_1+m_2)\eta}}{m_2}\end{array}\right)$$

$$+\frac{n_3}{n_2\left(n_3^2-n_2n_3\right)}\left(\frac{\lambda_1GrA^2e^{2\lambda_1\eta}}{\left(\lambda_1-n_2\right)}+\frac{\lambda_1GrABe^{(\lambda_1+\lambda_2)\eta}}{\left(\lambda_2-n_2\right)}+\frac{\lambda_1GcACe^{(\lambda_1+m_1)\eta}}{\left(m_1-n_2\right)}+\frac{\lambda_1GcADe^{(\lambda_1+m_2)\eta}}{\left(m_2-n_2\right)}\right)$$

$$-\frac{1}{\left(n_3^2-n_2n_3\right)}\left(\frac{\lambda_1GrA^2e^{2\lambda_1\eta}}{\left(\lambda_1-n_3\right)}+\frac{\lambda_1GrABe^{(\lambda_1+\lambda_2)\eta}}{\left(\lambda_2-n_3\right)}+\frac{\lambda_1GcACe^{(\lambda_1+m_1)\eta}}{\left(m_1-n_3\right)}+\frac{\lambda_1GcADe^{(\lambda_1+m_2)\eta}}{\left(m_2-n_3\right)}\right)\ ]+\ldots$$

$$\Phi_{1(p)}(\eta)=\frac{Sc}{(m_2-m_1)}\Big[\ m_1FCe^{(m_1+n_2)\eta}+m_1GCe^{(m_1+n_3)\eta}$$

$$-\left(\frac{n_3}{n_2\left(n_3^2-n_2n_3\right)}-\frac{1}{\left(n_3^2-n_2n_3\right)}\ \right)\left(\begin{array}{l}\dfrac{m_1GrACe^{(\lambda_1+m_1)\eta}}{\lambda_1}+\dfrac{m_1GrBCe^{(\lambda_2+m_1)\eta}}{\lambda_2}+GcC^2e^{2m_1\eta}\\ +\dfrac{m_1GcCDe^{(m_1+m_2)\eta}}{m_2}\end{array}\right)$$

$$+\frac{n_3}{n_2\left(n_3^2-n_2n_3\right)}\left(\frac{m_1GrACe^{(\lambda_1+m_1)\eta}}{\left(\lambda_1-n_2\right)}+\frac{m_1GrBCe^{(\lambda_2+m_1)\eta}}{\left(\lambda_2-n_2\right)}+\frac{m_1GcC^2e^{2m_1\eta}}{\left(m_1-n_2\right)}+\frac{m_1GcCDe^{(m_1+m_2)\eta}}{\left(m_2-n_2\right)}\right)$$

$$-\frac{1}{\left(n_3^2-n_2n_3\right)}\left(\frac{m_1GrACe^{(\lambda_1+m_1)\eta}}{\left(\lambda_1-n_3\right)}+\frac{m_1GrBCe^{(\lambda_2+m_1)\eta}}{\left(\lambda_2-n_3\right)}+\frac{m_1GcC^2e^{2m_1\eta}}{\left(m_1-n_3\right)}+\frac{m_1GcCDe^{(m_1+m_2)\eta}}{\left(m_2-n_3\right)}\right)\ \Big]+\ldots$$

$$-Gr\ \left\{\frac{\mathrm{J}_1e^{n_1\eta}}{n_2}+\frac{J_2e^{n_2\eta}}{n_2}\ +\frac{\mathrm{Pr}}{\left(\lambda_2-\lambda_1\right)}\left[\frac{\lambda_1FAe^{(\lambda_1+n_2)\eta}}{\left(\lambda_1+n_2\right)}+\frac{\lambda_1GAe^{(\lambda_1+n_3)\eta}}{\left(\lambda_1+n_3\right)}\right.\right.$$

$$-\left(\frac{n_3}{\left(n_3^2-n_2n_3\right)}-\frac{1}{\left(n_3^2-n_2n_3\right)}\right)\left(\frac{GrA^2e^{2\lambda_1\eta}}{2}+\frac{GrBAe^{(\lambda_1+\lambda_2)\eta}}{\left(\lambda_1+\lambda_2\right)}+\frac{\lambda_1GcCAe^{(\lambda_1+m_1)\eta}}{\left(\lambda_1+m_1\right)m_1}+\frac{\lambda_1GcDAe^{(\lambda_1+m_2)\eta}}{\left(\lambda_1+m_2\right)m_2}\right)$$

$$+\frac{n_3}{n_2\left(n_3^2-n_2n_3\right)}\left(\frac{GrA^2e^{2\lambda_1\eta}}{2\left(\lambda_1-n_2\right)}+\frac{\lambda_1GrBAe^{(\lambda_1+\lambda_2)\eta}}{\left(\lambda_2-n_2\right)\left(\lambda_1+\lambda_2\right)}+\frac{\lambda_1GcCAe^{(\lambda_1+m_1)\eta}}{\left(m_1-n_2\right)\left(\lambda_1+m_1\right)}+\frac{\lambda_1GcDAe^{(\lambda_1+m_2)\eta}}{\left(m_2-n_2\right)\left(\lambda_1+m_2\right)}\right)$$

$$-\frac{1}{\left(n_3^2-n_2n_3\right)}\left(\frac{GrA^2e^{2\lambda_1\eta}}{2\left(\lambda_1-n_3\right)}+\frac{\lambda_1GrBAe^{(\lambda_1+\lambda_2)\eta}}{\left(\lambda_2-n_3\right)\left(\lambda_1+\lambda_2\right)}+\frac{\lambda_1GcCAe^{(\lambda_1+m_1)\eta}}{\left(m_1-n_3\right)\left(\lambda_1+m_1\right)}+\frac{\lambda_1GcDAe^{(\lambda_1+m_2)\eta}}{\left(m_2-n_3\right)\left(\lambda_1+m_2\right)}\right)\ \Big]+\ldots\Big\}$$

$$f_{1(p)}(\eta)=\left(\frac{n_3}{n_2\left(n_3^2-n_2n_3\right)}-\frac{1}{\left(n_3^2-n_2n_2\right)}\right)\ \Big\{\ \Big[Fe^{n_2\eta}+Ge^{n_3\eta}$$

$$-\left(\frac{n_3}{n_2\left(n_3^2-n_2n_3\right)}-\frac{1}{\left(n_3^2-n_2n_3\right)}\ \right)\left(\frac{GrAe^{\lambda_1\eta}}{\lambda_1}+\frac{GrBe^{\lambda_2\eta}}{\lambda_2}+\frac{GcCe^{m_1\eta}}{m_1}+\frac{GcDe^{m_2\eta}}{m_2}\right)$$

$$+\frac{n_3}{n_2\left(n_3^2-n_2n_3\right)}\left(\frac{GrAe^{\lambda_1\eta}}{\left(\lambda_1-n_2\right)}+\frac{GrBe^{\lambda_2\eta}}{\left(\lambda_2-n_2\right)}+\frac{GcCe^{m_1\eta}}{\left(m_1-n_2\right)}+\frac{GcDe^{m_2\eta}}{\left(m_2-n_2\right)}\right)$$

$$-\frac{1}{\left(n_3^2-n_2n_3\right)}\left(\frac{GrAe^{\lambda_1\eta}}{\left(\lambda_1-n_3\right)}+\frac{GrBe^{\lambda_2\eta}}{\left(\lambda_2-n_3\right)}+\frac{GcCe^{m_1\eta}}{\left(m_1-n_3\right)}+\frac{GcDe^{m_2\eta}}{\left(m_2-n_3\right)}\right)\ ]+\ldots$$

$$-\frac{1}{\left(n_3^2-n_2n_3\right)}\left(\frac{GrAe^{\lambda_1\eta}}{\left(\lambda_1-n_3\right)}+\frac{GrBe^{\lambda_2\eta}}{\left(\lambda_2-n_3\right)}+\frac{GcCe^{m_1\eta}}{\left(m_1-n_3\right)}+\frac{GcDe^{m_2\eta}}{\left(m_2-n_3\right)}\right)\ ]$$

$$-\left(\frac{n_3}{\left(n_3^2-n_2n_3\right)}-\frac{1}{\left(n_3^2-n_2n_3\right)}\right)\left(\frac{GrA^2e^{2\lambda_1\eta}}{2}+\frac{GrBAe^{(\lambda_1+\lambda_2)\eta}}{\left(\lambda_1+\lambda_2\right)}+\frac{\lambda_1GcCAe^{(\lambda_1+m_1)\eta}}{\left(\lambda_1+m_1\right)m_1}+\frac{\lambda_1GcDAe^{(\lambda_1+m_2)\eta}}{\left(\lambda_1+m_2\right)m_2}\right)$$

$$+\frac{n_3}{n_2\left(n_3^2-n_2n_3\right)}\left(\frac{GrA^2e^{2\lambda_1\eta}}{2\left(\lambda_1-n_2\right)}+\frac{\lambda_1GrBAe^{(\lambda_1+\lambda_2)\eta}}{\left(\lambda_2-n_2\right)\left(\lambda_1+\lambda_2\right)}+\frac{\lambda_1GcCAe^{(\lambda_1+m_1)\eta}}{\left(m_1-n_2\right)\left(\lambda_1+m_1\right)}+\frac{\lambda_1GcDAe^{(\lambda_1+m_2)\eta}}{\left(m_2-n_2\right)\left(\lambda_1+m_2\right)}\right)$$

$$-\frac{1}{\left(n_3^2-n_2n_3\right)}\left(\frac{GrA^2e^{2\lambda_1\eta}}{2\left(\lambda_1-n_3\right)}+\frac{\lambda_1GrBAe^{(\lambda_1+\lambda_2)\eta}}{\left(\lambda_2-n_3\right)\left(\lambda_1+\lambda_2\right)}+\frac{\lambda_1GcCAe^{(\lambda_1+m_1)\eta}}{\left(m_1-n_3\right)\left(\lambda_1+m_1\right)}+\frac{\lambda_1GcDAe^{(\lambda_1+m_2)\eta}}{\left(m_2-n_3\right)\left(\lambda_1+m_2\right)}\right)\ ]$$

$$+\ldots\ -Gc\ \left\{\frac{\mathrm{R}_1e^{m_1\eta}}{m_1}+\frac{\mathrm{R}_2e^{m_2\eta}}{m_2}\ +\frac{Sc}{\left(m_2-m_1\right)}\left[\frac{m_1FCe^{(m_1+n_2)\eta}}{\left(m_1+n_2\right)}+\frac{m_1GCe^{(m_1+n_3)\eta}}{\left(m_1+n_3\right)}\right.\right.$$

$$\left(\frac{n_3}{n_2\left(n_3^2-n_2n_3\right)}-\frac{1}{\left(n_3^2-n_2n_3\right)}\right)\left(\frac{m_1GrACe^{\left(m_1+\lambda_1\right)\eta}}{\lambda_1\left(m_1+\lambda_1\right)}+\frac{m_1GrBCe^{\left(m_1+\lambda_1\right)\eta}}{\lambda_2\left(m_1+\lambda_1\right)}+\frac{GcC^2e^{2m_1\eta}}{2m_1}+\frac{m_1GcDCe^{\left(m_1+m_2\right)\eta}}{m_2\left(m_1+m_2\right)}\right)$$

$$-\frac{n_3}{n_2\left(n_3^2-n_2n_3\right)}\left(\frac{m_1GrACe^{\left(m_1+\lambda_1\right)\eta}}{\left(\lambda_1-n_2\right)\left(m_1+\lambda_1\right)}+\frac{m_1GrBCe^{\left(m_1+\lambda_2\right)\eta}}{\left(\lambda_2-n_2\right)\left(m_1+\lambda_2\right)}+\frac{GcC^2e^{2m_1\eta}}{\left(m_1-n_2\right)2}+\frac{m_1GcDCe^{\left(m_1+m_2\right)\eta}}{\left(m_2-n_2\right)\left(m_1+m_2\right)}\right)$$

$$-\frac{1}{\left(n_3^2-n_2n_3\right)}\left(\frac{m_1GrACe^{(m_1+\lambda_1)\eta}}{\left(\lambda_1-n_3\right)\left(m_1+\lambda_1\right)}+\frac{m_1GrBCe^{(m_1+\lambda_2)\eta}}{\left(\lambda_2-n_3\right)\left(m_1+\lambda_2\right)}+\frac{GcC^2e^{2m_1\eta}}{\left(m_1-n_3\right)2}+\frac{m_1GcDCe^{(m_1+m_2)\eta}}{\left(m_2-n_3\right)\left(m_1+m_2\right)}\right)\ ]$$

$+\ldots]\}$

$$E=0$$

$$F=\frac{\left(\ f_{o(p)}(0)e^{-(\mu_3+1/2)}-f_{o(p)}(1)\right)e^{1/2}}{2\sinh\mu_3},$$

$$G = \frac{-\left(\quad f_{o(p)}(0)e^{-(\mu_3+1/2)} - f_{o(p)}(1)\right)e^{1/2}}{2\sinh\mu_3} - f_{o(p)}(0)$$

$$J_1 = \frac{e^{\alpha x/2}\left(\gamma_1\Theta_w - \Theta_{1(p)}(\alpha x) + \Theta_{1(p)}(0)e^{-(\mu_1+1/2)\alpha x}\right)}{2\sinh(\mu_1\alpha x)}, \qquad J_2 = \frac{-e^{\alpha x/2}\left(\gamma_1\Theta_w - \Theta_{1(p)}(\alpha x) + \Theta_{1(p)}(0)e^{-(\mu_1+1/2)\alpha x}\right)}{2\sinh(\mu_1\alpha x)} - \Theta_{1(p)}(0)$$

$$R_1 = \frac{e^{\alpha x/2}\left(\gamma_2\Phi_w - \Phi_{1(p)}(\alpha x) + \Phi_{1(p)}(0)e^{-(\mu_2+1/2)\alpha x}\right)}{2\sinh(\mu_2\alpha x)},$$

$$R_2 = \frac{-e^{\alpha x/2}\left(\gamma_2\Phi_w - \Phi_{1(p)}(\alpha x) + \Phi_{1(p)}(0)e^{-(\mu_2+1/2)\alpha x}\right)}{2\sinh(\mu_2\alpha x)} - \Phi_{1(p)}(0)$$

© 2016 Okuyade and Abbey; This is an Open Access article distributed under the terms of the Creative Commons Attribution License (http://creativecommons.org/licenses/by/4.0), which permits unrestricted use, distribution, and reproduction in any medium, provided the original work is properly cited.

Peer-review history:
The peer review history for this paper can be accessed here:
http://sciencedomain.org/review-history/17370